Available online at www.sciencedirect.com
ScienceDirect
Bioelectrochemistry 70 (2007) 214–220
Bioelectrochemistry
www.elsevier.com/locate/bioelechem

Short communication

Antiproliferative effect of millimeter radiation on human erythromyeloid leukemia cell line K562 in culture: Ultrastructural- and metabolic-induced changes

A. Beneduci [a,b,*], G. Chidichimo [a,b], S. Tripepi [c], E. Perrotta [c], F. Cufone [b]

[a] Department of Chemistry, University of Calabria, Via P. Bucci Cubo 17/D 87036 Arcavacata di Rende (CS), Italy
[b] Consorzio TEBAID, c/o Department of Chemistry, University of Calabria, Via P. Bucci Cubo 17/C 87036 Arcavacata di Rende (CS), Italy
[c] Department of Ecology, Electron Microscopy Laboratory, Via P. Bucci Cubo 6/B University of Calabria, Arcavacata di Rende (CS), Italy

Received 24 May 2006; received in revised form 19 June 2006; accepted 7 July 2006
Available online 12 July 2006

Abstract

In the present study we compared the proliferation behavior, the ultrastructural morphology and the glycolitic metabolism of K562 cells irradiated by low-power wide-band millimeter waves, with those of sham-exposed K562 cells (control), maintained in the same culture conditions. The gigaHertz radiation treatments, performed between 53–78 10^9 Hz, induced a noticeable inhibition of the cell proliferation that could be related to relevant ultrastructural changes. Such effects brought the irradiated cell system to lose the homeostasis and to trigger defense/reparatory mechanisms in order to reestablish a new steady state. ^{13}C-Nuclear magnetic resonance data on the kinetic of glucose metabolism demonstrated that the irradiated cells enhanced the glycolitic aerobic pathway, indicating that such system need to produce an extra-bioenergy. Most of the ATP synthesized served probably to perform the above processes resulting in a significant decrease of the proliferation rate without significant cell death increment.

Keywords: Millimeter radiation; K562 cells; Cell proliferation; Cell ultrastructure; Glucose metabolism

1. Introduction

This work constitutes a further step of a study started at the beginning of the year 2000 whose aim was to understand the biological effects caused by low power (<10 mW/cm^2) electromagnetic radiation, in the millimeter wavelength range (3.84–5.78 mm), on some human cell systems either healthy or tumoral. Since 2002, we have shown that the electromagnetic radiation above mentioned, could be used as a physical mean in order to influence the proliferative behavior of the cultured cells [1]. The response to the radiation of the several cell systems investigated have been shown to be not the same. In particular, it should be underlined that all the tumoral systems investigated were negatively influenced by the millimeter radiation in certain exposure conditions, whereas the healthy cell systems studied were not [1]. Moreover, we have shown that the biological effects observed could depend not only on the cell system that interact with the radiation [1], but also on the frequency of the radiation and on the irradiation time [2]. Despite the low power of the millimeter waves used to irradiate the cells, significant morphological alterations were observed on human melanoma and human breast carcinoma cells [2,3].

The aim of this communication is to provide further biological evidences on the effects induced by the millimeter radiation on the K562 cell system cultured in vitro.

2. Experimental

2.1. Cell culture

K562 cells [4–7], human erythromyeloid leukemia cell line, obtained from the "Centro Studi della Microcitemia", (Cosenza), were grown at 37 °C in RPMI 1640, from Sigma, supplemented

* Corresponding author. Department of Chemistry, University of Calabria, Via P. Bucci Cubo 17/D 87036 Arcavacata di Rende (CS), Italy. Tel.: +39 0984492117; fax: +39 0984492041.
E-mail address: beneduci@unical.it (A. Beneduci).

1567-5394/$ - see front matter © 2006 Elsevier B.V. All rights reserved.
doi:10.1016/j.bioelechem.2006.07.008

with 10% (v/v) fetal calf serum, 50 U/ml penicillin, 50 μg/ml streptomycin, 20 mM Hepes and 0.85 g/l $NaHCO_3$, to adjust pH value to 7.2, in a fully humidified atmosphere of 5% CO_2 and 95% air. Cells from the stock flask were seeded at a density of 5×10^4 cell/plate into 35-mm culture dishes for cell proliferation and TEM observations and at a density of 5×10^5 cell/plate into 100-mm plates for NMR experiments.

Determination of the total cell count and viable cell number were made by the trypan blue exclusion essay with a hemocytometer. The mean cell counts came from three dishes for the treated and three dishes for the control sample. Differences between population means were considered significant at $p<0.5$.

2.2. Experimental MMW facilities and culture cell irradiation procedure

The radiation experiments were carried out through instruments produced by the UWOM company of Nizhny Novgorod (Russia). The MMW radiating apparatus, the AMFIT 32, is constituted by a microwave noise generator diode that is able to supply the frequency band 53.57–78.33 GHz at a global mean power density of less than 1 μW/cm^2. The electromagnetic radiation is irradiated into the free space by means of an opportune rectangular waveguide and a conical horn. The coupling between the millimeter radiation and the K562 cells was obtained by irradiating the cell system from the bottom of the culture dishes through the polystyrene base plate, placed inside the incubator at 37 °C.

The conical antenna was placed at a distance r sufficiently near to the Petri dishes that the radiation beam impinged the entire surface of the samples. In these situations, the far field conditions ($r>\lambda$) was always fulfilled too.

The cell system was irradiated 1 h every other day and the first irradiation started after the seeding. The control cell sample was cultured in the same culture conditions and was sham-exposed 1 h every other day too.

In the exposure conditions adopted, resonance phenomena eventually arising inside the incubator due to reflection of the waves by the metallic walls, were excluded for the following reasons:

i. the dimensions of the incubator (Cellstar 300; $47\times58\times47$ cm^3) are much greater than the wavelength of the radiation used (about from 3.8 to 5.8 mm);
ii. the reflections of the waves by the walls of the incubator were very small. In fact, our theoretical and experimental considerations on the coupling between the millimeter waves used and the aqueous media contained in commercial Petri dishes (unpublished results) show that about the 100% of the MMW transmitted into the sample through the polystyrene base plate of the Petri dishes, remained confined inside the aqueous medium. It is due either to the strong dispersive nature of water present in the culture system (medium+cells), that absorb the radiation at the millimeter frequencies used, or to the "infinite medium condition" (thickness of the sample much greater than the penetration depth of the radiation inside the medium ~ 0.3 mm) adopted in the in vitro experiments. Moreover, the most part of the incidence radiation is coupled (transmitted) into the aqueous medium.

2.3. Transmission electron microscopy

The cell suspensions at the 7th day of culture, after 4 MMW irradiation treatments (MMW-irradiated sample) or 4 sham-irradiation treatments (sham-exposed control sample), were centrifuged and the pellets were fixed with 3% glutaraldheyde solution (pH 7.3) for about 2 h at 4 °C. The cell suspensions were then rinsed twice with phosphate-buffer solution (PBS) and postfixed with 1% osmium tetraoxide solution (pH 7.3) and incubated for 2 h at 4 °C. The cells were then dehydrated in a graded series of alcohol for 5 min each. The dehydrated pellets were embedded three times with propylene oxide for 1 h each and infiltrated with a resin/propylene oxide mixture at 1:1 ratio for 2 h and then with resin only for 12 h at ambient temperature. The inclusion was made with Epon 812 and Araldite and the polymerization was performed at 60 °C for 48 h. Ultrathin sections were stained with uranyl acetate and counterstained with lead citrate. They were examined with the EM 900 Zeiss transmission electron microscope.

2.4. ^{13}C NMR measurements and data analysis

Magnetic resonance experiments were carried out on a Bruker MSL300 wide-bore spectrometer. A 10 mm high-resolution wide-band probe permitted the recording of ^{13}C spectra at 75.5 MHz. Spectra of 30 min resolution (900 scans) were obtained using 45° pulse and 2 s interpulse delay. Spin–spin coupling between ^{13}C–^{1}H nuclei was eliminated by applying continuous broad-band ^{1}H decoupling. Temperature of the samples inside the probe was maintained at 37±1 °C by the Bruker VT1000 variable temperature control unit.

Pellets of $0.8\div1\times10^8$ cells were resuspended in 1 ml of a 4% agarose/RPMI 1640 mixture, preheated at 40 °C to obtain the agarose melting (m.p.=37 °C). The new cell suspensions were

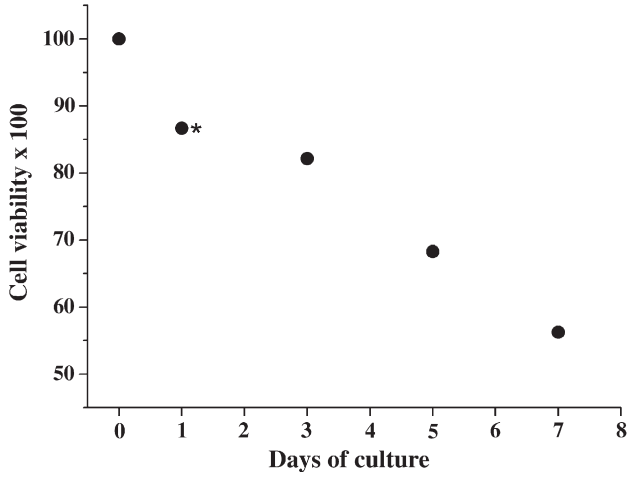

Fig. 1. Cell viability of the irradiated cells compared to that of the control cells as a function of the days of incubation. Cell viability=No. of MMW cells/No. of CTL cells. Student's t-test was adopted to asses the statistical significance of the data with 95% confidence interval ($N=3$). * No statistical significant difference ($p>0.05$).

injected by a syringe, into a teflon tube of 1.5 mm internal diameter and 100 cm long. After few minutes, agarose solidification took place and agarose/cell filaments could be extruded from the teflon tube directly into the 10-mm NMR tube containing the culture medium.

K562 cells entrapped in the agarose filaments, were oxygenated within the NMR probe, by a perfusion system that continuously provided to cells a O_2/CO_2 95% (v/v) gas mixture.

To monitor K562 glucose metabolism, 1-^{13}C-glucose (99% enrichment; Sigma) was added to the suspension to a final concentration of 5 mM. The NMR acquisitions were initiated immediately following such addition. Peak assignment of the ^{13}C resonances was based upon standard solutions as well as literature data [8]. Analysis of the K562 glucose metabolism were carried out by measuring the peak areas (peak intensities multiplied by the line width at half maximum peak intensities) of the ^{13}C-labeled metabolites in spectra processed with a line broadening of 10 Hz. For the quantification of ^{13}C-labelled metabolite peaks, the sum peak areas of the stereoisomer α-and β-^{13}C-glucose peak at their initial maximum intensity were taken to represent the known concentration of 1-^{13}C-glucose added. Metabolite peak areas in subsequent spectra were referenced to this initial value for the quantification of respective metabolites.

3. Results

3.1. Effect on K562 cell proliferation

Cell counts were made in triplicate 24 h after each irradiation treatment. In Fig. 1 the normalized viable cell number difference was reported as a function of the day of incubation. It was calculated by the formula:

$$\text{cell viability} = \frac{\text{No cells irradiated sample}}{\text{No cells control sample}} \times 100$$

The inhibitory effect induced by the MMW irradiation, evidenced by the decreasing trend of the above defined parameter,

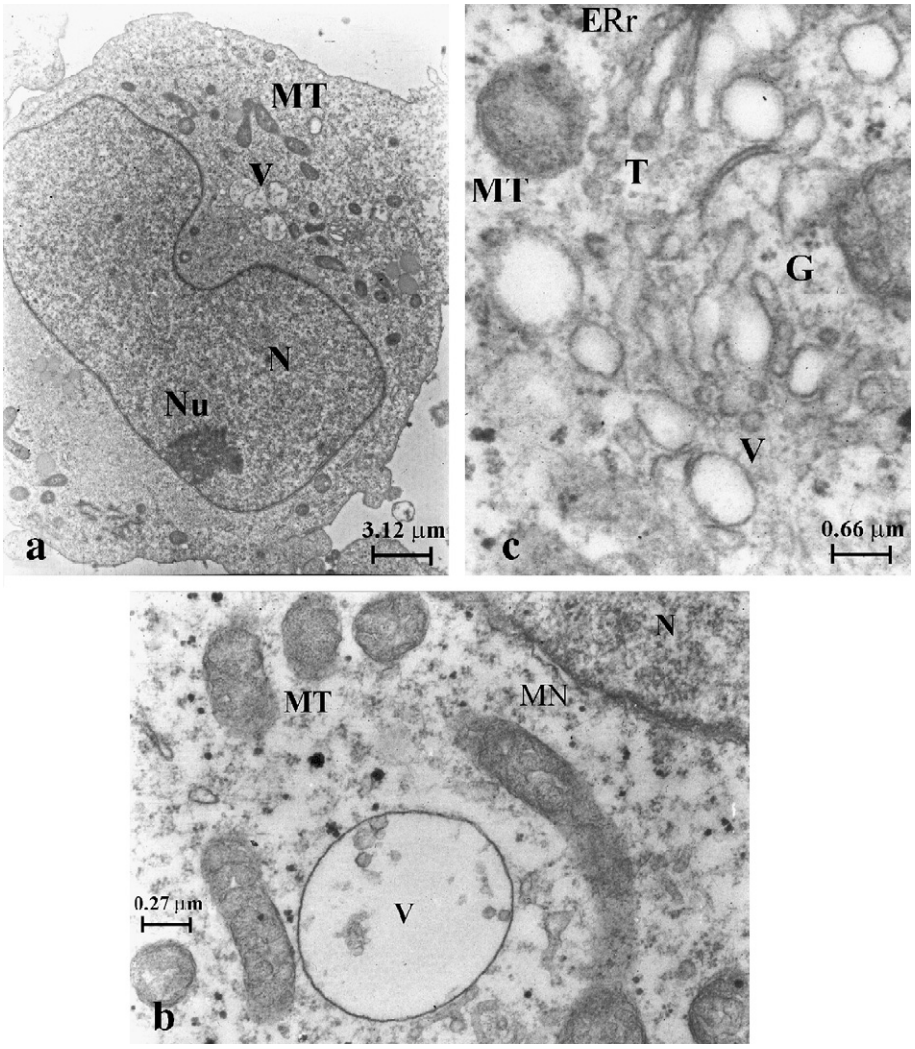

Fig. 2. Electron micrograph of control K562 cells: a) cell with a typical rounded morphology. Note the corrugations at its surface. Some mitochondria (MT) and vesicles (V) are visible within the cytoplasm. The nucleus (N) contains either euchromatin or heterochromatin (original magnification ×4400); b) zoom of the cytoplasm containing either spherical or oblate mitochondria (original magnification ×20000); c) Golgi complex (G) with transition vesicles (T) and a small portion of rough endoplasmic reticulum (ERr) in its vicinity (original magnification ×30000).

Table 1
Average number of mitochondria/cell in ultrathin section (Nm) and percentage of vesicle-containing cells (%Cells), for control (CTL) and irradiated (MMW) K562 samples

	CTL	MMW
Nm	35±7	58±9
Nv	%Cells	%Cells
0–5	82±8	24±2
6–15	18±2	29±3
16–50	0	27±3
>50	0	20±2

The number of vesicles (Nv) was arbitrarily subdivided into four intervals. The error margins represents the standard deviation calculated on a count performed on 100 cells.

was related to the number of irradiation treatments, thus to the global radiative energy given to the cells. After 4 irradiation treatments, the number of viable cells in the treated samples was significantly reduced by over 40% with respect to the sham-exposed sample. It should be noted that there was no significant difference in the number of dead cells between the two samples.

3.1.1. Ultrastructure of the non-irradiated control K562 cells

The ultrastructural characteristics of non irradiated control K562 cells, as revealed by TEM observation of the ultrathin sections, are shown in the electron photomicrographs reported in Fig. 2. Control cells were generally round but their surface was characterized by many corrugations and microvilli-like structures. The cytoplasm contained a relatively abundant number of mitochondria often with large dimensions (Table 1; Fig. 2). Such organelles assumed either spherical or rod-like morphology, and presented clearly visible cristae (Fig. 2).

The great majority of control cells contained few cytoplasmic vesicles (0–10) (Fig. 2; Table 1).

The cytoplasm also possessed an extended rough endoplasmic reticulum with ribosomes. It could be noted also an improved Golgi apparatus. The secretory–endocytic traffic was evidenced

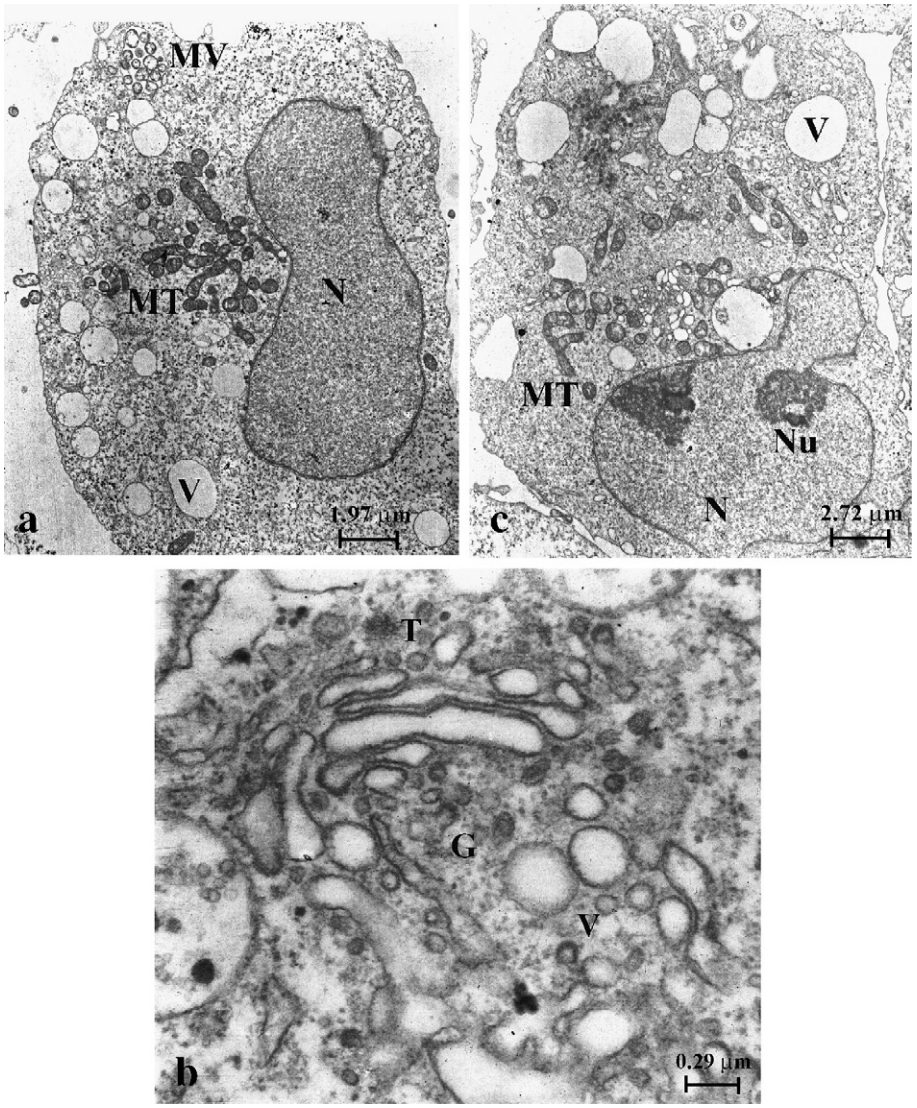

Fig. 3. Electron micrograph of K562 cells after four MMW-irradiation treatments of 1 h each: a) and c) K562 cells in which a high number of vesicles (V) and mitochondria (MT) addensation were observed; also visible is a multivesicular body (MV) (original magnification ×7000, a,c; ×4400); b) cytoplasm containing an improved Golgi complex (G) with transition vesicles (T) (original magnification ×30000). Nucleus (N); nucleoli (Nu).

by the presence of transition vesicles (T) located between the rough endoplasmic reticulum (ERr) and the cis Golgi complex (G) and by vesicles of greater dimensions (V) that gemmated from the trans face of the Golgi apparatus (Fig. 2).

Nucleus of sham-exposed control K562 cells showed indentation or lobate morphology and it occupied an extended portion of the cytoplasm as it was also observed by optical microscopy. One or two nucleoli were generally found. Either dispersed chromatin (euchromatin) or condensed one (heterochromatin) were observed. Heterochromatin was found preferentially at the periphery of the nucleus (Fig. 2).

3.1.2. Ultrastructure of the MMW-irradiated K562 cells

The MMW-irradiated cells were round with few corrugations and microvilli. These finding appears to agree with our previous scanning electron microscopy report [1], though a correct interpretation could be affected by the centrifugation procedures adopted to prepare the samples for TEM observation.

A count performed on the ultrathin sections revealed that the cytoplasm of the treated cells, contained a higher number of mitochondria with respect to the sham-exposed sample (Table 1). The count, either for control or MMW-irradiated samples, was made selecting 20 cells per thin section for 5 different sections, for a total of 100 cells.

In many cases, a high density of mitochondria were found in the region between the nucleus, the granular endoplasmic reticulum and the Golgi complex (Fig. 3). The ERr was found to be very electrondense (high number of ribosome) and the Golgi apparatus well developed (Fig. 3).

No variation in the mitochondria morphology were found between control and irradiated samples.

A very distinctive feature of the MMW-irradiated cells, was the high number of cytoplasmic vesicles found (Table 1; Fig. 3). In Table 1 the % of vesicles-containing cells were reported subdividing arbitrarily the No. of vesicles (Nv) to be found in the cells, into four intervals. In the CTL sample, the greatest number of vesicles found was 15 with more than 80% of cells containing only very few vesicles (0–5). By contrast, in the MMW sample, about the 55% of cells contained a No. of vesicles ≤ 15, while the other 45% a higher number of such structures.

In some cases, multivesicular bodies were also noted (Fig. 3).

The nucleus of the treated cells was characterized by indentation and contained finely dispersed chromatin with a small fraction of heterochromatin. On the other hand, 1–2 prominent nucleoli were generally noted (Fig. 3).

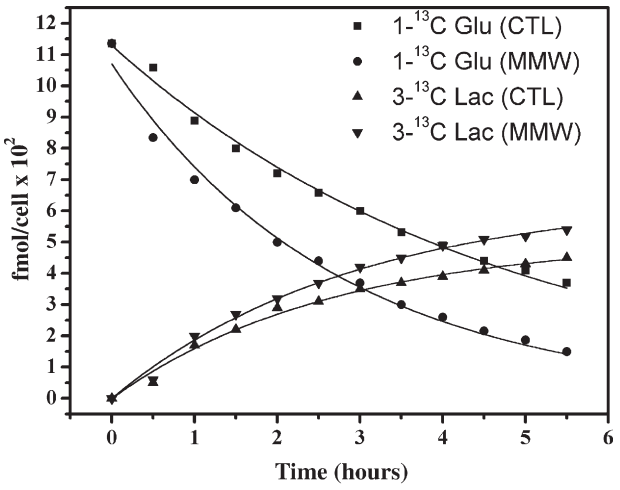

Fig. 4. 1-^{13}C-glucose consumption and 3-^{13}C-lactate labelling in samples of control and MMW-irradiated K562 cells. Each point represent the glucose or lactate concentration (fmol/cell) calculated from the intensities of the peaks of a single spectrum from the entire series. Solid lines represent the best exponential fit of the data points. The rate constants of glucose consumption and lactate production for the two samples are reported in Table 2.

Table 2
Kinetics of 1-^{13}C-glucose consumption and 3-^{13}C-lactate production found in control (CTL) and irradiated (MMW) K562 cells samples

	1-^{13}C-glucose consumption fmol/(cell/h)	3-^{13}C-lactate synthesis fmol/(cell/h)
CTL	0.212±0.005	0.377±0.042
MMW	0.367±0.014	0.342±0.040

Values represent the mean±SD (N=3).

3.2. Glucose metabolism

In Fig. 4 the kinetics of glucose consumption and lactate formation were shown for the control (CTL) and irradiated (MMW) K562 cell system together whit the best exponential fits (solid lines). Such kinetics were best modeled using a non linear least square analysis to obtain an exponential fit of the metabolite concentration data over a time-course of at least 5,5 h. The following equations were used to fit the data for respectively, glucose consumption and lactate production: $y = A\ e^{-k\ t}$; $y = A\ (1 - e^{-k\ t})$. Table 2 gives the exponential curve fitting results.

In the analysis of the spectra, the measures of the peak areas took into account a correction factor for the Nuclear Overhauser Enhancement (NOE) or partial saturation effects which arise from, respectively, the continuous ^{1}H-decoupling and the short interpulse interval used during data acquisition. Correction factors from literature data were used [9].

From the above ^{13}C NMR data one could see that the MMW-irradiated system significantly increase the glucose consumption with respect to the control sample, without significantly effecting the kinetic of lactate labeling. This metabolic change had to reflect an enhancement of the glycolytic aerobic pathway as a response of the cells to the radiative treatments. The increase in the number of mitochondria and the mitochondria addensation could be morphological evidences that well relates to the latter conclusion.

4. Discussion

Cell count made on the irradiated and sham-exposed samples at the 7th day of culture, revealed a significant 40% reduction of the number of cells in the first sample. This experiment confirms the inhibitory effect of the wide-band low-power millimeter wave radiation on the proliferation of K562 cells in culture, as we previously observed [1].

The picture that emerged from TEM observation on the ultrathin sections of the MMW-irradiated K562 cells, was that of a system in a high energy metabolic state far from "equilibrium" steady state (homeostasis). The increase of mitochondria respiration must be interpreted as a need by the cell not only to produce more energy but also that glycolytic anaerobic pathway was not able to adequately provide the bioenergetic request. Such argument was supported by the ^{13}C NMR results that indicated an intense aerobic glycolysis performed by the treated cells. Moreover, we saw that mitochondria were preferentially concentrated in the region near the nucleus, the ERr and the Golgi complex, probably because in this region the cell needed more energy to perform protein synthesis. In addition, MMW-irradiated cells presented improved substructures such as nucleoli, euchromatin and ERr, that play crucial role in the synthesis of ribosomes, RNA and protein respectively.

Finally, the irradiated system exhibited an abnormal quantity of cytoplasmic vesicles. The nature of such vesicles most probably resembles that involved in degenerative cellular processes [10].

Then, on one hand the irradiated cell lose its homeostasis because of the irradiation, giving rise to proliferation decrement and some morphological alterations pertinent to cellular degenerative processes. On the other hand, the irradiated cell tried to establish a new steady state (autoadaptation), producing more energy and triggering the activity of subcellular structures and processes as a sort of defense-reparatory mechanism. The injuries induced by the radiation appeared to be reversible otherwise, a significant cell death increment between the two samples should have to be observed.

Trying to delineate a mechanism responsible of the observed effects, we believe that any plausible physico-chemical interpretation must involve the water present in the biological system as a very probable primary target of the millimeter waves. Water is a strong absorber of the radiation at these frequencies. Actually, the dielectric dispersion curve of pure water at 20 °C is centred at 20 GHz (corresponding to a relaxation time of about 8 ps) and extend over 100 GHz [11,12]. The dynamics of rotation and libration of water molecular dipoles are responsible of such a dielectric behaviour. Moreover, it is generally accepted that at microwave frequencies (above 10^9 Hz), the dielectric behaviour of tissues, cells as well as protein solutions, is dominated by the relaxation process of water [13–18]. Actually, the electric properties of these systems could be expressed by logarithmic frequency dependence over the whole frequency range from few Hertz to many gigaHertz. At microwave frequencies the electric properties are characterized by two dispersion regions called δ and γ. The dominant γ dispersion is due to the bulk water (also free water) and is identical to that of pure water. It falls approximately in the range 10^9–10^{11} Hz. The other dispersion region, δ, falls in the range $10^8 \div 10^9$ Hz. It was attributed by Schwan et al. [13–15] to arising in part from Maxwell–Wagner effects due to the electrolyte content of the tissues, in part from dielectric relaxation in the protein itself and in part from rotational relaxation of its bound water. Such dispersion was also attributed by Grant et al. to the protein-bound water in studies on protein in solution [16–18].

Recently, microwave dielectric dispersion measurements, have shown that at least three relaxation times other than that of free water, could be attributed to water in a biopolymer solution. Each correlation time corresponds to a different water structure with decreasing mobility. In the order: bound water, structured water and loosely structured water [19].

Taking into account these considerations, one has driven to conclude that the MMW interact principally with the free water present in the cells.

However, as it has been underlined by Neumann [20], besides the direct field effect on water dipoles (in our case), any biological effects could be explained only if the electromagnetic field affects the reaction sensitivity of some cellular processes, that is crucially determined by the reaction moments.

The absorption of microwave radiation by water molecules may induce changes in the equilibrium free water/bound water involved in several cellular processes in which a chemical control is exerted. For instance, a key reaction process of this type, is a bimolecular reaction of ligand binding coupled to conformational changes of the receptive effector molecules and to the release of water molecules from the hydration shells of the ligand and binding sites (that are ionic or dipolar and hence, hydrated) of the reaction partners [20].

Water plays also crucial roles in proton transfer reactions and in transport processes through narrow channels or pores in which water molecules assume particular interfacial orientations [20]. The millimeter radiation could affect the orientational dynamics of water molecules in such systems.

Acknowledgement

This work has been supported by the Lega Italiana per la Lotta Contro i Tumori Sezione Cosenza.

References

[1] G. Chidichimo, A. Beneduci, M. Nicoletta, M. Critelli, R. De Rose, Y. Tkachenko, S. Abonante, S. Tripepi, E. Perrotta, Selective inhibition of tumoral cells growth by low power millimeter waves, Anticancer Res. 22 (2002) 1681–1688.
[2] A. Beneduci, G. Chidichimo, R. De Rose, L. Filippelli, S.V. Straface, S. Venuta, Frequency and irradiation time-dependant antiproliferative effect of low-power millimeter waves on RPMI 7932 human melanoma cell line, Anticancer Res. 25 (2005) 1023–1028.
[3] A. Beneduci, G. Chidichimo, S. Tripepi, E. Perrotta, Transmission electron microscopy study of the effects produced by wide-band low-power millimeter waves on MCF-7 human breast cancer cells in culture, Anticancer Res. 25 (2005) 1009–1014.
[4] C.B. Lozzio, B.B. Lozzio, Human chronic myelogenous leukemia cell-line with positive Philadelphia chromosome, Blood 45 (1975) 321–334.
[5] E. Klein, H. Ben-Bassat, H. Neumann, P. Ralph, J. Zeuthen, A. Polliack, F. Vanky, Properties of the K562 cell line, derived from a patient with chronic myeloid leukaemia, Int. J. Cancer 18 (1976) 421–431.
[6] B.B. Lozzio, C.B. Lozzio, Properties of the K562 cell line, derived from a patient with chronic myeloid leukaemia, Int. J. Cancer 19 (1977) 136.
[7] L. Anderson, K. Nilsson, C. Gahmber, K562-human erytroleukemic cell line, Int. J. Cancer 23 (1979) 143–147.
[8] P. Canioni, J. Alger, R.G. Shulman, Natural abundance carbon-13 nuclear magnetic resonance spectroscopy of liver and adipose tissue of the living rat, Biochemistry 22 (1983) 4976–4980.

[9] J.F.M. Post, E. Baum, E.L. Ezell, ^{13}C NMR studies of glucose metabolism in human leukemic CEM-C7 and CEM-C1 cells, Magn. Reson. Med. 23 (1992) 356–366.
[10] R. Munker, L. Greither, M. Darsow, S. Pander, W. Wilmanns, TNF induced cytoplasmic vesicles in actinomycin D-treated K562 cells, Ann. Hematol. 65 (1992) 50–52.
[11] U. Kaatze, The dielectric spectrum of water in the microwave and near-millimeter wavelength region, Chem. Phys. Lett. 132 (1986) 291–293.
[12] H.J. Liebe, G.A. Hufford, T. Manabe, A model for the complex permittivity of water at frequencies below 1 THz, Int. J. Infrared Millim. Waves 12 (1991) 659–675.
[13] K.R. Foster, L. Schepps, H.P. Schwan, Microwave dielectric relaxation in muscle. A second look, Biophys. J. 29 (1980) 271–282.
[14] H.P. Schwan, Dielectric properties of biological tissue and cells at RF-and MW-frequencies, in: S.M. M.Grandolfo, A. Michaelson (Eds.), Biological effects and dosimetry of non ionizing radiation. NATO Advanced Study Institutes Series. Series A, Life Sciences, Plenum Press, New York, 1983, pp. 195–211.
[15] ∅.G. Martinsen, S. Grimnes, H.P. Schwan, Interface phenomena and dielectric properties of biological tissues, Enciclopedia of Surface and Collloid Science, Marcel Dekker, Inc., 2002, pp. 2643–2652.
[16] E.H. Grant, A.G.P. South, S. Takashima, H. Ichimura, Dielectric dispersion in aqueous solutions of oxyhaemoglobin and carboxyhaemoglobin, Biochem. J. 122 (1971) 691–699.
[17] C.G. Essex, M.S. Symonds, R.J. Sheppard, E.H. Grant, R. Lamote, F. Soetewey, M.Y. Rosseneu, H. Peeters, Five-component dielectric dispersion in bovine serum albumin solution, Phys. Med. Biol. 22 (1977) 1160–1167.
[18] E.H. Grant, Molecular interpretation of the dielectric behaviour of biological materials, in: M. Grandolfo, S.M. Michaelson, A. Rindi (Eds.), Biological effects and dosimetry of non ionizing radiation. NATO Advanced Study Institutes Series. Series A, Life Sciences, Plenum Press, New York, 1983, pp. 179–193.
[19] K. Yoshiba, A. Teramoto, N. Nakamura, Water structures of differing order and mobility in aqueous solutions of Schizophyllan, a triple-helical polysaccharide as revealed by dielectric dispersion measurements, Biomacromolecules 5 (2004) 2137–2146.
[20] E. Neumann, Digression on chemical electromagnetic field effects in membrane signal transduction−cooperativity paradigm of the acetylcholine receptor, Bioelectrochemistry 52 (2000) 43–49.